DESIGN AND CONTROL OF A PASSIVELY STEERED, DUAL AXLE VEHICLE

Michael Wagner, Stuart Heys, David Wettergreen, James Teza, Dimitrios Apostolopoulos, George Kantor, William Whittaker

The Robotics Institute, Carnegie Mellon University, Pittsburgh, PA 15213, USA,
Email: {mwagner, sheys, dsw, jpt, da1v, kantor, red}@ri.cmu.edu

ABSTRACT

In this paper we describe the steering, suspension and control systems of the rover Zoë, a solar-powered robot designed to explore the Mars-like landscapes of the Atacama Desert in Chile. We are developing the Zoë chassis as an alternative to the traditional six-wheeled, rocker-bogie system used by Mars rovers flown in the past ten years. Zoë travels over rough terrain using only four independent drive motors. Steering is accomplished by differentially driving pairs of these motors to passively articulate front and rear steering axles. In this paper we present a detailed mechanical design of the chassis, a description of Zoë's steering controller and results of steering controller tests that validate this design. We also include lessons learned after field experiments in the Atacama Desert of Chile.

1. INTRODUCTION

Eight years ago, a Mars rover was something that could drive very slowly between rocks within a few meters of its landing site. Now, a Mars rover is being designed that will be capable of wandering to its own horizon every few days and of visiting hundreds of sites over several years.

We believe that this fundamental change in role necessitates a re-evaluation of Mars rover chassis design. A chassis that works well for a small, Sojourner-class rover may not be appropriate for rovers with wheel diameters larger than Sojourner itself.

The six-wheeled rocker-bogie design [1] demonstrated on Mars by the Sojourner rover. The rocker-bogie chassis is intended to allow a vehicle with small wheels to climb over obstacles much larger than its wheel radius. Tight maneuvers such as point turns are achieved with independent steering of four of its six wheels. Because of its linkages, six wheel modules and four steering motors, the rocker-bogie design has a significantly higher part count, mass and complexity than a more traditional 4WD chassis. Taking on extra mass and complexity is worthwhile for a small vehicle to gain more obstacle climbing ability. Sojourner's wheels were only 13 cm in diameter [2], while the expected obstacle distribution reflected in a "Mars yard" test bed, included rocks as large as 60 cm [3]. The extra maneuverability also allowed Sojourner to get close to rocks for science investigations.

Yet as rovers grow larger and travel further, the costs of a rocker-bogie suspension begin to outweigh the benefits. For example, the Mars rover planned for a mission in 2009 is expected to have wheels that are 70 cm in diameter. Even without a suspension, a simple 4WD vehicle with the same wheels could climb over obstacles 35 cm high. MSL will be mechanically capable of driving over rocks one to two meters high, but the advantage of doing this is not clear. If fewer tight turns are required, there is also little benefit from the extra mass of steering motors.

The rocker-bogie suspension could actually limit the mobility of tomorrow's wayfaring Mars rover. A rocker-bogie has problems driving through natural terrain at human walking speeds. Its front wheels must climb vertically up the leading edge of an obstacle to surmount it. This can bring the vehicle itself to a halt and impose large forces on its frame [4]. Analyses have also shown the maximum slope-climbing ability of rocker-bogies to be more limited than standard 4WD vehicles [5].

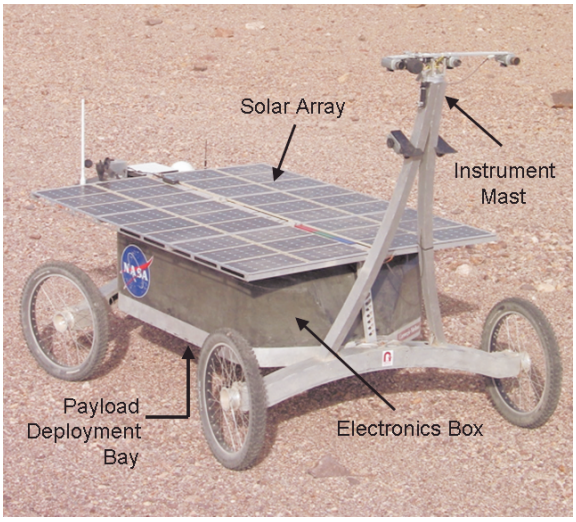

Fig. 1: Zoë in the Atacama Desert.

Proc. 'ISAIRAS 2005 Conference', Munich, Germany,
5-8 September 2005 (ESA SP-603, September 2005)

This paper explores an alternative chassis design that is minimalist yet fully capable and appropriate for an autonomous, long-range Mars rover traveling at speeds up to 100 cm/s. This chassis uses front and rear steering axles that are articulated passively by driving wheel motors differentially. An averaging mechanism along the chassis' roll axis distributes the vehicle's weight equally amongst all four wheels. This suspension system, passive like a rocker-bogie, also improves obstacle climbing ability.

We have built a rover called Zoë to study this new design. Zoë is a solar-powered rover designed to explore the Mars-like landscapes of the Atacama Desert in Chile (see Fig. 1). Zoë traveled 50 km autonomously through the desert in a search for life that was overseen by a team of remote scientists operating as if the robot were on Mars [6].

2. CHASSIS OVERVIEW

Two competing factors motivated the design of the Zoë chassis. First, Zoë was intended to traverse long distances over desert terrain at roughly human walking speeds. Its travels would take it beyond the field of view of any panoramic image, so it must be prepared to avoid or surmount obstacles and slopes without human intervention. Reliability is therefore a key metric. Furthermore Zoë is built to survey large geological units, not to study specific rocks. Therefore it has neither an instrument arm nor a need to make very tight turns.

The second motivation was minimizing Zoë's power consumption because the rover is entirely solar powered. This argues for a minimalist, low mass design with low part count and fewer degrees of freedom.

Naturally these motivations conflict with each other. But the Zoë design does a good job at satisfying our goals of both reliably traversing rough desert terrain while keeping power consumption low. Zoë uses four independently driven wheels. The vehicle steers by driving its wheels differentially, causing its passive steering joints to pivot. Fig. 2 depicts the Zoë chassis in several configurations. Zoë achieves higher maneuverability by steering both axles symmetrically, unlike our previous rover Hyperion [7] which had a single steering axle. The body length identical for both Hyperion and Zoë, but with axle(s) set to 20 degrees, Hyperion travels an arc of about 5.5-m radius while Zoë travels an arc of about 2.7-m radius.

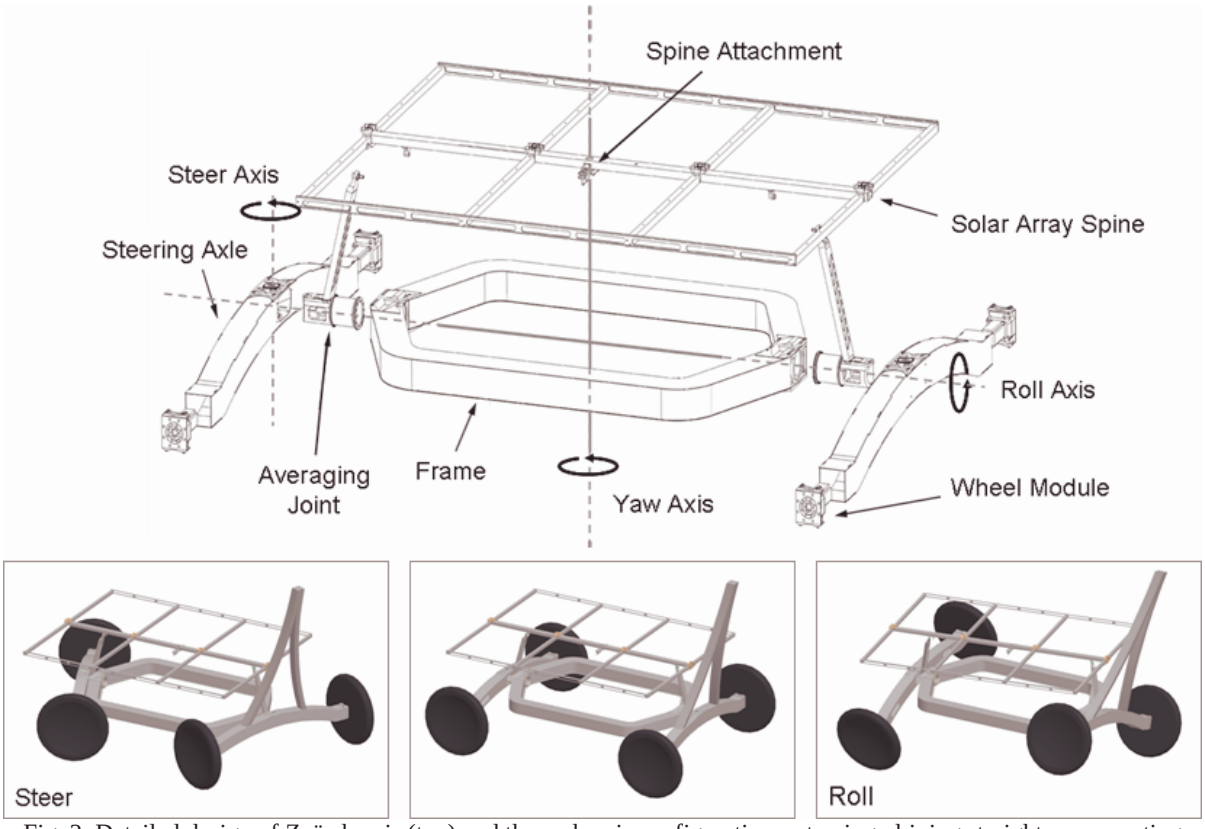

Fig. 2: Detailed design of Zoë chassis (top) and three chassis configurations: steering, driving straight, surmounting rough terrain (bottom, left to right).

A suspension system is a necessity for a vehicle such as Zoë; steering and control of the vehicle depend on all four wheels being in continuous contact with the ground. If each wheel carries a similar load, performance over difficult terrain improves since the likelihood of a single wheel slipping is minimized. A passively suspended, averaged chassis like Zoë's can address both of these problems while minimizing the complexity and mass of the system.

Zoë's chassis carries a 2.4 m^2 solar array, 0.32 m^3 of electronics, a forward-leaning instrument mast on the front axle and a science payload deployment bay in the chassis center. This bay includes the fluorescence imager deployment mechanism as well as a plow to dig a shallow subsurface trough. Size and mass characteristics are summarized in Table 1.

Mass breakdown:
GVW: 198 kg
Chassis: 36 kg
Other mechanical components: 69 kg
Electrical components and payload: 93 kg
Wheelbase: 1.63 m
Maximum speed: 110 cm/s
Wheel radius: 37.5 cm
Minimum turning radius: 2.5 m
Ground clearance:
Near wheels: 35 cm
Chassis center: 40 cm

Table 1: Zoë chassis characteristics.

The design also has the practical benefit of being easy to disassemble and re-assemble in the field. The electronics enclosure is split into two halves, both of which lift out of the hexagonal frame. The axles can also be detached for easy shipping.

3. CHASSIS AVERAGING AND SUSPENSION

Similar in many ways to the averaged chassis of the Nomad rover [8], the roll angle of Zoë's frame with respect to the ground is always the average of the roll angles of the two steering axles. The roll angles of each axle with respect to the frame are always symmetrically opposite. This improves the rover's weight distribution while on uneven terrain since the chassis sees a more or less equal excursion when any of the four tires encounters an obstacle. While Nomad's averaging, like that of MER or Sojourner, is performed over a transverse axis through the rover, Zoë's is about a longitudinal axis. This configuration allows averaging to be implemented without interfering with the rover's steering and also without many extra parts.

The top of Fig. 2 illustrates the subassemblies that comprise Zoë's chassis: two steering axles that each contain two wheel modules, two averaging joints, a hexagonal frame that supports the electronics enclosure and the solar array spine and hinged solar array halves. Each axle has a freedom around a "steer" axis (parallel to the yaw axis) that is implemented with a pair of thin section bearings. These joints are referred to as averaging joints because they also include a rotational joint through the roll axis of the vehicle. This is also implemented with thin section bearings, allowing cabling to pass from within the axles directly into the electronics enclosure. Each averaging joint includes a near vertical member, the roll mast, which attaches to the underside of the solar spine via a spherical bearing. The chassis and electronics enclosure is supported by the roll bearings which transfer the load through the steering joints and into the axles. To constrain the roll degree of the chassis, the solar spine is attached through the central yaw axis of the chassis.

The bottom right of Fig. 2 shows Zoë at an extreme roll angle, the equivalent of a single wheel surmounting a 1.3-m obstacle. To eliminate the need for an explicit averaging link and the many degrees of freedom required in the three attachment points of that link as in Nomad's averaging system, Zoë depends on the flexing of several components to compensate for the dimensional changes forced on the frame as Zoë traverses obstacles. This method, though eventually limited by the yield strength of the flexing components, requires very few additional parts and adds little complexity or weight to the system. As the averaging joints roll with respect to each other, the distance between the tops of the roll masts increases slightly. This change is absorbed by the flexing of these two parts towards the centre of the robot. Spherical bearings at the tops of the masts account for the angular changes between the roll mast and the solar array. Since the tops of the roll masts follow an arc as the axles roll, their position with respect to the chassis becomes lower as roll angle increases, imposing a downward force on the solar spine. Lastly, a rotational joint connects the solar spine to the center of the electronics box, through the central yaw axis of the rover.

4. TRACTION AND WHEEL MODULES

Enclosed within the ends of each axle are four wheel modules (see Fig. 3). Each wheel module consists of a brushless drive motor connected to a 100:1 ratio harmonic drive. The output of the harmonic drive is supported through an output flange which also provides an attachment point for the wheel hub. This flange is supported by a preloaded four point contact bearing that absorbs wheel loads but is stiff enough to

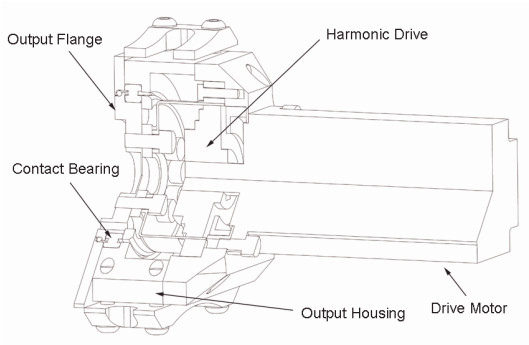

Fig. 3: Wheel module cutaway.

keep the harmonic drive components in alignment. The entire assembly is contained in a sealed aluminium output housing which also provides a mounting point to the axle. Table 2 lists the commercially available components used in the wheel module design.

Drive motor:	Kollmorgen AKM 22 G
Harmonic drive:	HD Systems CSF-25-100-2A-GR
Contact bearing:	Kaydon JB025XP0

Table 2: Wheel module components.

The simplicity of the wheel module makes it compact and lightweight. The assembly weighs less than 2.75 kg total and fits within a 100 mm x 100 mm x 200 mm opening at the end of the axle. The harmonic drive gearing and high quality servomotor can intermittently generate over 200 N-m of driving torque.

Zoë's wheels use 3-inch wide pneumatic tires. Steel spokes connect the rim to a custom machined hub with a bolt pattern to match that of the output flange. The assembly is extremely strong and relatively lightweight at 3 kg. Pneumatic tires are effective in the Atacama Desert although for Mars or lunar exploration a different flexible tire design would be more appropriate.

The steepest grade that Zoë can drive is limited by the traction of the wheels rather than by its drive torque capacity. When the wheels grip the terrain well, Zoë is able climb high vertical steps. Fig. 4 shows one such test we performed with the chassis before adding the full electronics box and solar panels. In this situation Zoë was able to drive its front end up an approximately 1.4-m vertical step. Fortunately, our obstacle avoidance software can very reliably avoid such situations.

5. LOCOMOTION POWER

The power transferred to each drive motor's amplifier was logged during two weeks of testing in the Atacama Desert. Hall effect sensors were sampled by an A/D


Fig. 4: A lightly-loaded Zoë chassis pulling itself up a 1.4-m vertical step.

converted connected to a PC/104 computer on the robot. This computer was dedicated to power sensing and logged the one-second average reading from each of the four sensors.

An analysis of these logs found that the locomotion system consumed on average 260 W of power throughout these weeks. Note that this measurement includes inefficiencies of the amplifiers. Over these two weeks Zoë drove over many different terrains: flat plains, rock-strewn fields and sandy slopes. Therefore this average is more characteristic of the entire region of the Atacama Desert than of a particular terrain type.

The energy consumed by the drive motors was small enough so that Zoë could also use its payload for science operations without draining its batteries. On average, the rover's collected almost 2750 W-hr of solar energy each day while consuming 2560 W-hr.

Fig. 5 depicts the relationship between distance traveled and locomotion energy. Statistics are presented for each of the twelve days with complete power logs. The figure shows distance traveled with blue bars, locomotion energy with the green bars. The blue line represents the ratio of energy per unit distance traveled. On average, 148 W-hr were required for Zoë to drive one kilometer through the Atacama Desert. The standard deviation of this ratio was 39 W-kr/km. Deviations from the average are likely due to traveling through terrain that is consistently smooth or rough. The most energy efficient driving occurred on October 14. On that day Zoë was traveled 3.3 km autonomously in a single command cycle. This area was relatively flat with obstacles more like boulders than trenches. Zoë's obstacle avoidance system is proficient at avoiding boulder-type obstacles so it was able to maintain a safe, flat path for the rover.

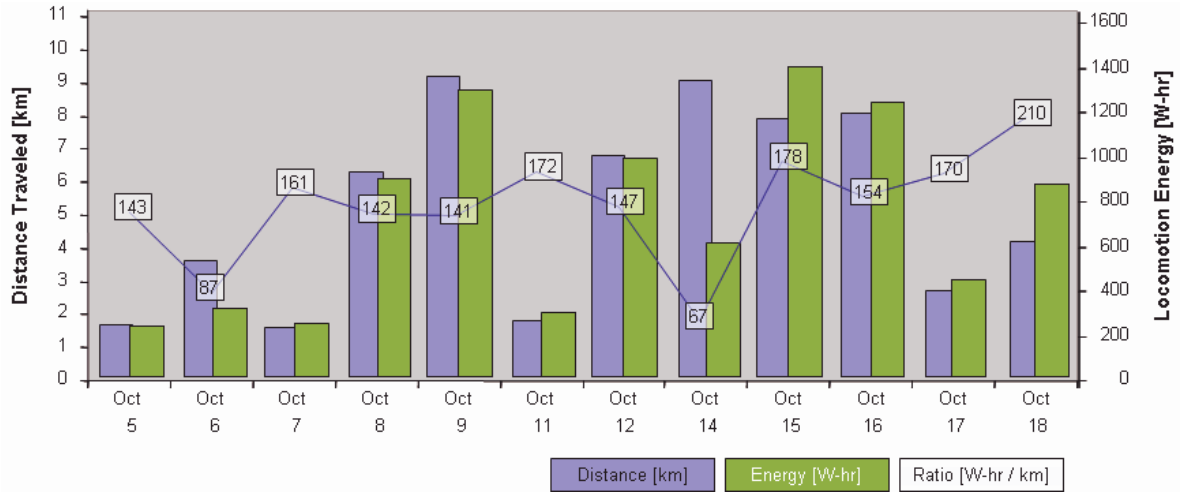

Fig. 5: Analysis of the relationship between distance traveled and energy consumed by locomotion.

6. KINEMATIC ANALYSIS

There is a one-to-one mapping from the chassis' configuration to the resulting path radius. The path radius is determined by finding the point of intersection of lines extended from each steering axle. Unfortunately many different steer axle angles can bring about a given arc path.

Ideally the steering angle of the front axle is symmetric to that of the rear, having the same magnitude but the opposite sign. In any other configuration, more range of motion is needed to achieve the same path radius. A visual explanation can be found in Fig. 6. On the left side of the figure, the steer angles are symmetric and the robot is driving along an arc with radius R_{robot}. On the right side, the steer angles are not symmetric: the front is under-steered while the rear is over-steered. Compared to the symmetric configuration, the asymmetric configuration requires a wider range of axle rotation is necessary to drive a given path.

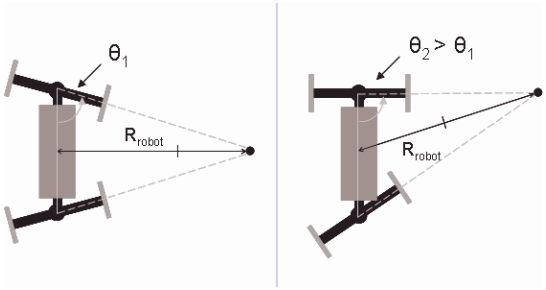

Fig. 6: Symmetric steering angles (left) provide more maneuverability for a limited range of steering axle motion than do other configurations (right).

7. STEERING BEHAVIOR

Initial steering tests showed that the chassis tends towards incorrect configurations, like that shown on the right of Fig. 6. This occurs after recovering from obstacle climbing or when driving any curved path.

To overcome these effects we implemented closed-loop feedback control on the steering axle angles. Although proportional feedback on the steering axle angles does reduce errors, a very predictable steady-state error remains. The front steer axle under-steers and the rear axle over-steers. At fast speeds or on tight turns, the rear axle steers so much as to force a wheel against the electronics box.

We observed that the steady-state error is a function of the magnitude of the commanded steer angle, the commanded robot velocity and the proportional gain of the feedback loop. As an example, consider the case when Zoë is commanded to drive at 50 cm/s with a 10-degree steering axle angle. Our tests show that the front steer axle settles at about 21 degrees while the rear axle settles at about -7 degrees. The steady-state steer error is not due to an axle's intrinsic characteristics (e.g. frictions within steer pivots) but whether the axle is leading or trailing.

We measured this steady state error by performing a number of tests. In each test we issued to the robot a driving command consisting of a desired velocity and steering axle angle. The proportional gain remained constant for all tests. The tests covered commands to drive the robot forward, reverse, to the left, to the right and straight. In all 90 tests were performed. The details are given in [9] but are summarized here.

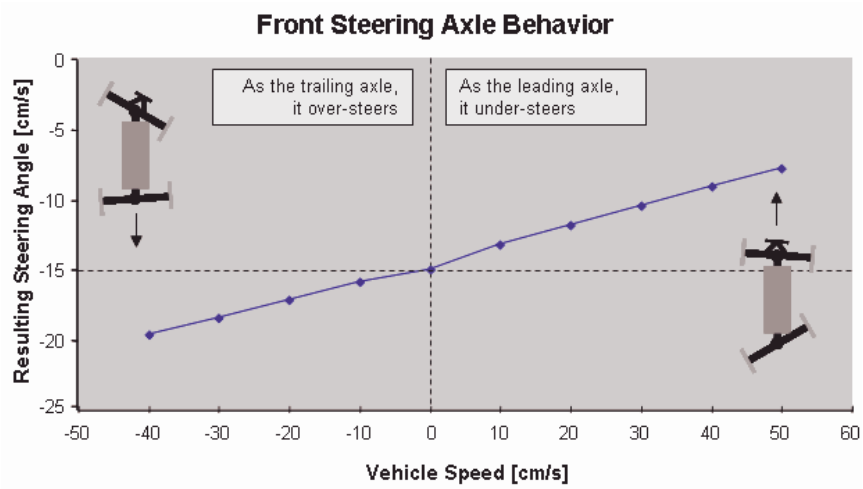

Fig. 7: One set of results from front steering axle calibration. The commands were to set the steering axles at 15 degrees to the right, while the commanded velocity ranged from 40 cm/s reverse to 50 cm/s forward.

First, we modeled the relationship between velocity and steer error for a given commanded steer angle. These relationships turned out to be very linear for speeds less than 80% of top vehicle speed. Below this threshold, the steer errors were proportional to velocity. Above this threshold, fewer data could be taken since the axle would drive into the electronics box more readily. We linearly modeled the behavior at these speeds as well, but with a large slope. Note that the vehicle drives in reverse the behavior of the axles is swapped.

We collected these linear functions for a number of commanded steering axle angles from -20 degrees (a tight left turn) to 20 degrees (a tight right turn). Not surprisingly, we found that the behavior of right turns is equivalent to that of left turns.

One set of calibration results for the front steering axle is shown in Fig. 7. The data in the figure show how the steady-state front steer angle changes when the vehicle is commanded to a 15-degree steer angle at different velocities. Note that as speed increases in the forward direction, the front axle under-steers more noticeably. When the vehicle moves backwards, the axle is trails and over-steers. Notice that around 50 or 60 cm/s in reverse, the axle will reach its maximum safe steering angle.

8. CONTROLLER DESIGN

A controller that successfully corrected these steady state errors is depicted in Fig. 8. Stages of the controller are organized from left to right, starting with the kinematic model (shown in blue). This block converts path radii to steer angles as described above in Section 6.

Next, the controller uses a feedforward term (shown in green) to cancel out over- and under-steering effects. The predictable nature of the steady-state steer angle errors favors a feedforward control term rather than integral feedback because it is not prone to instability problems.

The feedforward term takes as inputs the desired steering angle and nominal wheel velocity. The first step of the feedforward block constrains the front and rear steer angles to be symmetric. Next, it takes the inverse of the model described in Section 7 that predicts steady-state steer angle error based on commanded speed and steering angle. Based on this model, the feedforward term calculates what angles should be used as a set point to the feedback loops to achieve the desired steering angles.

These set points become inputs to two steering angle feedback loops (shown in yellow). One loop controls the front steering axle, one loop controls the rear. Each loop outputs a differential wheel velocity term for its axle, shown as $\Delta\omega$ in the figure. This differential velocity is added to one wheel and subtracted from the other wheel on the axle, which rotates the axle towards the commanded angle. The $\Delta\omega$ command is proportional to the difference between the actual steer angle and the fed-forward steer angle command.

At the lowest level of the controller (shown in red), velocity control is performed on each wheel by dedicated, multi-axis motion control hardware (a Galil DMS-2182 multi-axis controller with Kollmorgen amplifiers). Encoder values are differenced to measure actual wheel velocity. Control signals are generated with a PID controller running on the dedicated microcontroller.

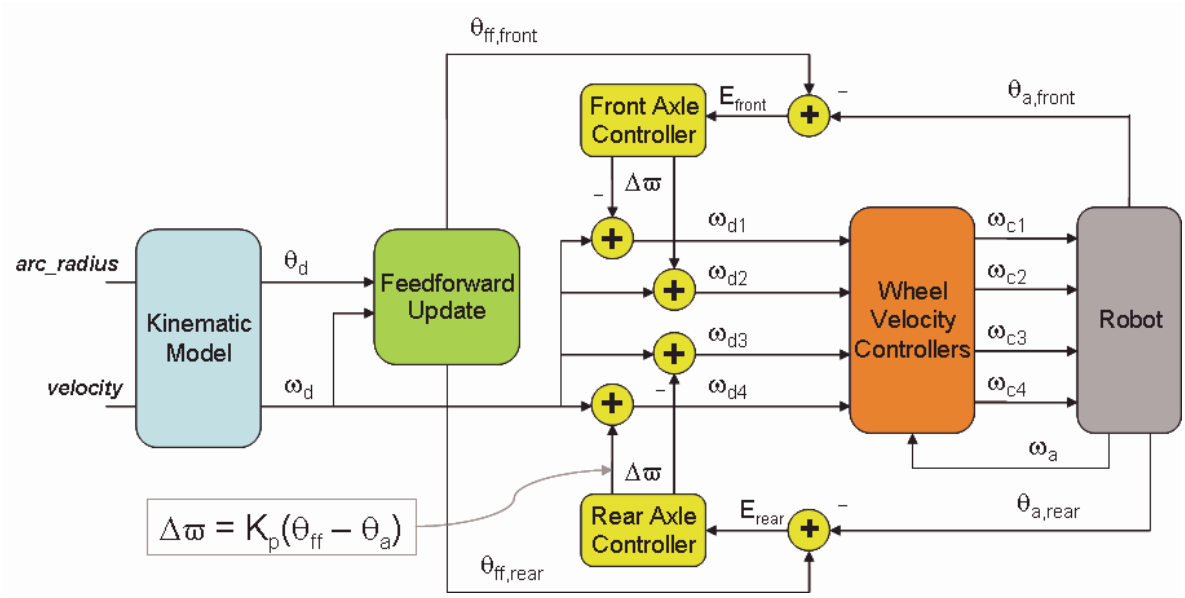

Fig. 8: Diagram of a steering controller for the passively articulated, dual axle chassis. The controller uses both feedforward (green) and feedback (yellow) blocks.

9. LIMITATIONS

Without steering actuators it is impossible to guarantee that Zoë will not fall into an improper chassis configuration. For instance, an axle may over-steer and run a wheel into the electronics box. Impaired control may result from rapid perturbations (e.g. running a wheel into any obstacle at high speed) or impassable terrain (e.g. running a wheel into a hopelessly large obstacle, or losing traction on soft soils).

We assume that impassable terrain can be avoided by obstacle avoidance software, which sends commands to the steering controller. Therefore we take a fail-safe approach rather than attempt automatic recoveries in the steering controller. If either steering axle angle exceeds a threshold, vehicle motion is stopped. This keeps the vehicle from being damaged, although it places the burden of avoiding these types of failures on the obstacle avoidance software.

This approach is valid for the case of impassable obstacles, but is less valid in the case of lost soil traction. The obstacle avoidance layer is not yet capable of detecting soft soils, so currently it cannot avoid this terrain. If traction is lost, the steering controller becomes ineffective, and the vehicle will usually stop due to axle angle thresholds being exceeded.

A dual axle, passively steered vehicle can continue to drive if one or two wheel modules on the same axle fail electrically. If the wheel is still able to be back driven, then both wheels on the axle can be switched off and allowed to be back drive. The vehicle can then continue to drive, but it must drive in the direction of the failed axle.

10. LESSONS LEARNED AND FUTURE WORK

Zoë's chassis proved to be successful in overcoming many terrain hazards presented by the Atacama Desert. In all, Zoë traveled more than 100 km across two desert sites in September and October of 2004. Approximately 50 km of this was performed under the control of Zoë's autonomy software.

A few types of terrain were particularly treacherous for Zoë's chassis. The cohesion of soil on slopes in the Atacama varies. In some cases, the tires can maintain good traction with the soil, even on slopes larger than 20 degrees. At other locations, the soil is nothing but fine, gypsum powder and on these slopes the tires lose traction at around 10 degrees. We hope to improve Zoë's performance in these situations using heuristics about how to climb soft slopes. For instance, if controller error limits or steer limits are exceeded, Zoë could attempt to climb the slope again but at a lower speed. At lower speeds we expect the vehicle to suffer less slip. We are also considering a wider wheel designs that would provide better flotation.

Another difficult terrain feature is a large vertical step such as the sides of a dried river bed or railroad (although the latter are not expected on Mars). Fig. 9 shows one such feature that could be as high as one meter. When Zoë approaches these steps from the low

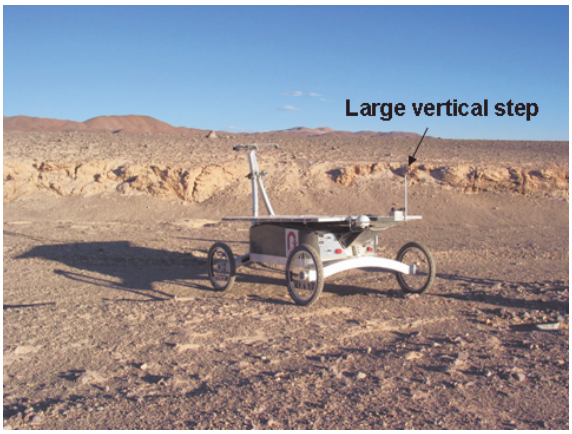

Fig. 9: Zoë approaching a large vertical step at the side of a dried river bed.

side, its obstacle avoidance software is effective, but these features can extend for hundreds of meters and impede progress. The more dangerous situation occurs when Zoë approaches a vertical step from the high side, where obstacle detection is more difficult. Solving this problem requires more intelligent processing of sensor data, such as methods proposed in [10].

Our ongoing work also includes improving Zoë's steering control. One important goal is to analytically derive the model used by our feedforward controller. Empirically building this model requires running dozens of tests over the course of several hours.

We also want to extend our kinematic model and controller from two dimensions to three. This requires accounting for the roll angle with respect to the chassis center of each axle. This would provide a better model of obstacle climbing and may improve controller response in these cases.

11. ACKNOWLEDGEMENTS

This paper describes the work of the Life in the Atacama project to which all members have made important contributions. Specifically, the authors would like to thank Dominic Jonak, Christopher Williams, Allan Lüders and Francisco Calderón for their helpful discussions and assistance in testing. We also thank the NASA Astrobiology Science and Technology for Exploring the Planets (ASTEP) program, David Lavery, Program Executive and Michael Meyers, Program Scientist.

12. REFERENCES

1. D. Bickler, US Patent Number 4,840,394 - Articulated Suspension Systems, US Patent Office, Washington, D.C., 1989.
2. R. Manning, "Mars Pathfinder FAQs – Sojourner", web page available online at http://mpfwww.jpl.nasa.gov/MPF/rover/faqs_sojourner.html
3. R. Volpe, J. Balaram, T. Ohm and R. Ivlev, "The Rocky 7 Mars Rover Prototype", *proceedings of IROS 1996*, pp. 1558-1564
4. D. P. Miller and T. Lee, "High-Speed Traversal of Rough Terrain Using a Rocker-Bogie Mobility System", *proceedings of Robotics 2002: The 5th International Conference and Exposition on Robotics for Challenging Situations and Environments*, Albuquerque, New Mexico, March 2002.
5. M. Thainwiboon, V. Sangveraphunsiri and R. Chancharoen, "Rocker-Bogie Suspension Performance", *Proceedings of he Eleventh International Pacific Conference in Automotive Engineering (IPC-11)*, November 6-9, 2001. Shanghai China.
6. D. Wettergreen, N. Cabrol, V. Baskaran, F. Calderon, S. Heys, D. Jonak, A. Luders, D. Pane, T. Smith, J. Teza, P. Tompkins, D. Villa, C. Williams, M. Wagner, "Second Experiments in the Robotic Investigation of Life in the Atacama Desert of Chile", *to appear in the Proceedings of i-SAIRAS 2005*.
7. B. Shamah, M. D. Wagner, S. Moorehead, J. Teza, D. Wettergreen, and W. L. Whittaker, "Steering and Control of a Passively Articulated Robot", *SPIE, Sensor Fusion and Decentralized Control in Robotic Systems IV*, Vol. 4571, October, 2001.
8. E. Rollins, J. Luntz, A. Foessel, B. Shamah, and W. Whittaker, "Nomad: A Demonstration of the Transforming Chassis", *proceedings of the Intelligent Components for Vehicles*, March, 1998.
9. M. Wagner, "Zoë Chassis Design Document", webpage is available online at http://www.fieldrobotics.org/atacama/zoe-chassis/
10. A. Avedisyan, D. Wettergreen, T. W. Fong, and C. Baur, "Far-field terrain evaluation using geometric and toposemantic vision", *Workshop on Advanced Space Technologies for Robotics and Automation (ASTRA)*, ESA, November 2004.